J|A|C|S
ARTICLES
Published on Web 02/15/2007

Nonstatistical Behavior of Reactive Scattering in the $^{18}O+^{32}O_2$ Isotope Exchange Reaction

Annalise L. Van Wyngarden,*[,†,#] Kathleen A. Mar,[†] Kristie A. Boering,*[,†,‡] Jim J. Lin,[§] Yuan T. Lee,[§,||] Shi-Ying Lin,[⊥] Hua Guo,[⊥] and Gyorgy Lendvay[○]

Contribution from the Department of Chemistry, University of California, Berkeley, California 94720, Department of Earth and Planetary Science, University of California, Berkeley, California 94720, Institute of Atomic and Molecular Sciences, Academia Sinica, Taipei, Taiwan, Department of Chemistry, National Taiwan University, Taipei, Taiwan, Department of Chemistry, University of New Mexico, Albuquerque, New Mexico 87131, and Chemical Research Center, Hungarian Academy of Sciences, Budapest, Hungary

Received September 21, 2006; E-mail: avanwyngarden@arc.nasa.gov; boering@berkeley.edu

Abstract: The recombination of oxygen atoms with oxygen molecules to form ozone exhibits several strange chemical characteristics, including unusually large differences in formation rate coefficients when different isotopes of oxygen participate. Purely statistical chemical reaction rate theories cannot describe these isotope effects, suggesting that reaction dynamics must play an important role. We investigated the dynamics of the $^{18}O + {}^{32}O_2 \rightarrow O_3^* \rightarrow {}^{16}O + {}^{34}O_2$ isotope exchange reaction (which proceeds on the same potential energy surface as ozone formation) using crossed atomic and molecular beams at a collision energy of 7.3 kcal mol^{-1}, providing the first direct experimental evidence that the dissociation of excited ozone exhibits significant nonstatistical behavior. These results are compared with quantum statistical and quasi-classical trajectory calculations in order to gain insight into the potential energy surface and the dynamics of ozone formation.

Introduction

Statistical theories of chemical reaction rates have been largely successful in describing and estimating thermal rate coefficients for a variety of unimolecular and bimolecular reactions.[1] The fundamental tenet of statistical theories for complex-forming reactions is that energy flow in an energized collision complex is significantly faster than dissociation to products so that energy is randomly redistributed in the complex, any memory of how the complex formed is lost, and the initial conditions are therefore irrelevant for predicting how the complex proceeds to products, thus greatly simplifying the calculations. Reactions that cannot be unambiguously modeled with statistical theories—for example, those in which dynamics must be explicitly accounted for due to an energy transfer bottleneck and/or a very fast dissociation rate[2]—are thus of both fundamental and practical interest.[3]

An intriguing example in which dynamics likely plays an important role is the recombination of oxygen atoms and molecules to form ozone (O_3).[4,5] In particular, extremely large and unusual kinetic isotope effects (KIEs) have been observed.[6,7] Marcus and co-workers[8] reproduced the relative isotope-specific formation rate coefficients using Rice−Ramsperger−Kassel−Marcus (RRKM) theory, showing how small zero-point energy (ZPE) differences between various isotopologues of O_2 reactants could be amplified into large KIEs, but only when an empirical nonstatistical (i.e., dynamically driven) factor was included. Quasi-classical trajectory calculations[9−12] that included isotope-specific ZPEs also revealed a nonstatistical effect since some trajectories formed an excited ozone complex (O_3*) but dissociated before energy was randomized, with the magnitude depending on the specific isotopes involved.[11,12] Babikov and

[†] Department of Chemistry, University of California.
[‡] Department of Earth and Planetary Science, University of California.
[§] Academia Sinica.
[||] National Taiwan University.
[⊥] University of New Mexico.
[○] Hungarian Academy of Sciences.
[#] Present address: Atmospheric Science Branch, NASA Ames Research Center, Moffett Field, CA 94035, USA.

(1) Baer, T.; Hase, W. L. *Unimolecular Reaction Dynamics, Theory and Experiments*; Oxford University Press: New York, 1996.
(2) Schinke, R.; Keller, H. M.; Flothmann, H.; Stumpf, M.; Beck, C.; Mordaunt, D. H.; Dobbyn, A. J.; Rice, S. A.; Marcus, R. A.; Troe, J.; Neumark, D. M.; Kellman, M. E. *Adv. Chem. Phys.* **1997**, *101*, 745−787.
(3) Gruebele, M.; Wolynes, P. G. *Acc. Chem. Res.* **2004**, *37*, 261−267.
(4) Mauersberger, K.; Krankowsky, D.; Janssen, C.; Schinke, R. *Adv. At., Mol., Opt. Phys.* **2005**, *50*, 1−54.
(5) Schinke, R.; Grebenshchikov, S. Y.; Ivanov, M. V.; Fleurat-Lesard, P. *Annu. Rev. Phys. Chem.* **2006**, *57*, 625−661.
(6) Janssen, C.; Guenther, J.; Krankowsky, D.; Mauersberger, K. *J. Chem. Phys.* **1999**, *111*, 7179−7182.
(7) Mauersberger, K.; Erbacher, B.; Krankowsky, D.; Gunther, J.; Nickel, R. *Science* **1999**, *283*, 370−372.
(8) Gao, Y. Q.; Marcus, R. A. *Science* **2001**, *293*, 259−263.
(9) Schinke, R.; Fleurat-Lesard, P. *J. Chem. Phys.* **2005**, *122*, 094317.
(10) Schinke, R.; Fleurat-Lesard, P.; Grebenshchikov, S. Y. *Phys. Chem. Chem. Phys.* **2003**, *5*, 1966−1969.
(11) Fleurat-Lesard, P.; Grebenshchikov, S. Y.; Siebert, R.; Schinke, R.; Halberstadt, N. *J. Chem. Phys.* **2003**, *118*, 610−621.
(12) Fleurat-Lesard, P.; Grebenshchikov, S. Y.; Schinke, R.; Janssen, C.; Krankowsky, D. *J. Chem. Phys.* **2003**, *119*, 4700−4712.

10.1021/ja0668163 CCC: $37.00

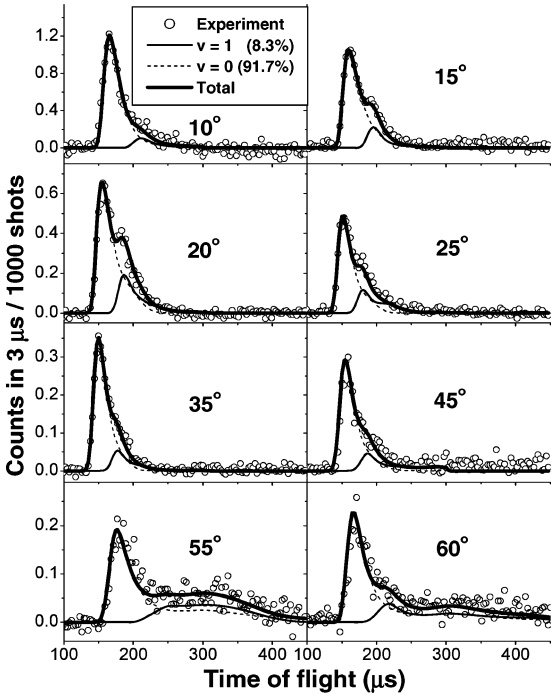

Figure 1. Time-of-flight spectra for $m/z = 34$ ($^{18}O^{16}O$) at eight different laboratory angles. Note different *y*-axis scales. Open circles are the experimental data; solid lines are the empirical simulation.[22]

co-workers[13] performed full quantum reactive scattering calculations for formation of various O_3* isotopologues that may qualitatively explain the ZPE dependence of the formation rate coefficients but which were limited to total angular momentum $J = 0$ due to computational constraints. A full quantum treatment, including O_3* formation, dissociation, and collisional stabilization,[14] is clearly beyond current capabilities. One means of circumventing this problem is to experimentally probe and model only the O_3* formation and dissociation steps through oxygen isotope exchange reactions

$$X + YZ \leftrightarrow XYZ^* \rightarrow XY + Z \qquad (1)$$

in which X, Y, and Z can be any combination of ^{16}O, ^{17}O, and ^{18}O. This reaction proceeds on the same $O_3(X^1A')$ potential energy surface (PES) as that for ozone formation and also exhibits unusually large isotope effects.[12,15] While thermally averaged rate coefficients have been measured and modeled for several isotopic variants of Reaction 1 (11, 12, 15−17), the dynamics have not been directly investigated experimentally. Here, we report experimental reactive scattering results for the $^{18}O(^3P) + {}^{32}O_2(^3\Sigma_g^-) \rightarrow {}^{16}O(^3P) + {}^{34}O_2(^3\Sigma_g^-)$ reaction and compare the results to predictions from two approximate theoretical methods, a quantum statistical (QS) model[18,19] (which includes quantum effects such as tunneling and zero-point energies) and quasi-classical trajectory (QCT) calculations. These results directly demonstrate the nonstatistical behavior of O_3* and provide insight into the O_3 PES and the applicability of statistical and approximate dynamical theories for describing O_3* dissociation.

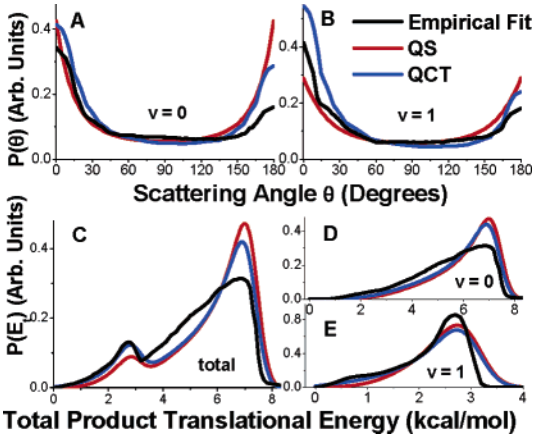

Figure 2. Product angular and translational energy distributions used to empirically simulate the data (black) and from QS and QCT predictions (red and blue, respectively). (A) $v = 0$ $P(\theta)$. (B) $v = 1$ $P(\theta)$. (C) Total $P(E_t)$. (D) $v = 0$ $P(E_t)$. (E) $v = 1$ $P(E_t)$ (note different *y*-axis scale).

Results and Discussion

The angular and velocity distributions of the $^{34}O_2$ product resulting from collisions of $^{18}O(^3P)$ with $^{32}O_2$ were measured using a universal crossed-molecular beam apparatus.[20,21] An atomic beam of 50% $^{18}O(^3P)$ and 50% $^{18}O(^1D)$ was crossed with a molecular beam of $^{32}O_2$ at a collision energy, E_{coll}, of 7.3 ± 0.5 kcal/mol ($\pm 2\sigma$), and the time-of-flight (TOF) spectra of the product $^{34}O_2$ were measured at various laboratory angles. The background-corrected TOF spectra (Figure 1, symbols) reveal two peaks that we assign to isotope exchange on the $O_3(X^1A')$ PES: a main peak corresponding to $^{34}O_2$ produced in its ground vibrational state ($v = 0$) and a second peak (or a shoulder on the $v = 0$ peak depending on laboratory angle) corresponding to the first vibrationally excited state ($v = 1$). Collisions of $O(^1D)$ with O_2 are not expected to contribute (see methods section below).

To extract center-of-mass (COM) product energy and angular information, the TOF spectra were fit empirically (Figure 1, lines) using an iterative forward-convolution method[23] in which trial COM product angular and translational energy probability distributions ($P(\theta)$ and $P(E_t)$, respectively) were used to simulate the TOF spectra accounting for machine parameters, beam characteristics, and the COM-to-lab-frame conversion. Two channels with separate $P(\theta)$s and $P(E_t)$s for $^{34}O_2$ in $v = 0$ and $v = 1$ were included in the fits (Figure 2). Two important characteristics are immediately apparent. First, the best-fit total

(13) Babikov, D.; Kendrick, B. K.; Walker, R. B.; Pack, R. T.; Fleurat-Lesard, P.; Schinke, R. *J. Chem. Phys.* **2003**, *118*, 6298−6308.
(14) The studies cited assume ozone formation proceeds via the energy transfer mechanism: $O + O_2 \rightarrow O_3^*$ and $O_3^* + M \rightarrow O_3 + M$. However, analysis of kinetics data,[35] supported by recent classical trajectory calculations,[36] suggests that at 298 K there may be a non-negligible contribution from the "chaperon" mechanism: e.g., $O + M \rightarrow O\bullet\bullet M$ and $O\bullet\bullet M + O_2$ proceeding to $O_3 + M$.
(15) Anderson, S. M.; Hülsebusch, D.; Mauersberger, K. *J. Chem. Phys.* 1997, *107*, 5385−5392.
(16) Yeh, K. -L.; Xie, D.; Zhang, D. H.; Lee, S. -Y.; Schinke, R. *J. Phys. Chem. A* **2003**, *107*, 7215−7219.
(17) Lin, S. Y.; Guo, H. *J. Phys. Chem. A* **2006**, 110, 5305−5311.
(18) Rackham, E. J.; Gonzalez-Lezana, T.; Manolopoulos, D. E. *J. Chem. Phys.* **2003**, *119*, 12895−12907.
(19) Lin, S. Y.; Guo, H. *J. Chem. Phys.* **2004**, *120*, 9907−9910.
(20) Perri, M. J.; Van Wyngarden, A. L.; Lin, J. J.; Lee, Y. T.; Boering, K. A. *J. Phys. Chem. A* **2004**, *108*, 7995−8001.
(21) Lin, J. J.; Hwang, D. W.; Harich, S.; Lee, Y. T.; Yang, X. *Rev. Sci. Instrum.* **1998**, *69*, 1642−1646.
(22) The ratio of the $v = 1$ to $v = 0$ channels was set to that predicted by the QS model. Changing the ratio alters the $P(E_t)$s and $P(\theta)$s slightly but does not change any of the conclusions.
(23) Lin, J. J.; Harich, S.; Lee, Y. T.; Yang, X. *J. Chem. Phys.* **1999**, *110*, 10821−10829.

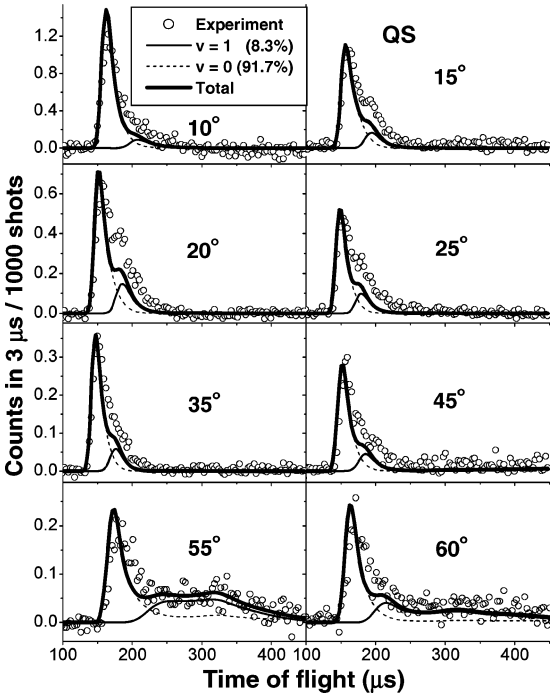

Figure 3. Time-of-flight spectra for $m/z = 34$ ($^{18}O^{16}O$) (open circles) and the QS prediction (solid lines). Note different *y*-axis scales.

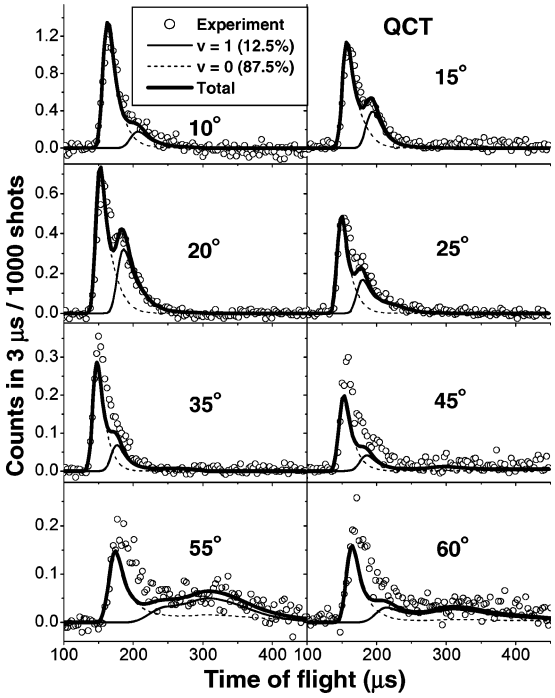

Figure 4. Time-of-flight spectra at $m/z = 34$ ($^{18}O^{16}O$) (open circles) and the QCT prediction (solid lines). Note different *y*-axis scales.

$P(E_t)$ (i.e., for $v = 0 + v = 1$ in Figure 2C) peaks near the collision energy limit, indicating minimal rovibrational excitation of the $^{34}O_2$ product. Second, the best-fit $P(\theta)$s for $v = 0$ and $v = 1$ (Figure 2A,B) are forward/backward peaking but biased toward the forward direction. Forward/backward symmetric scattering results from collisions that proceed through complexes that are long-lived relative to their rotational periods and are expected to behave statistically. Thus, this forward scattering bias indicates that the reaction has some nonstatistical character. This conclusion is robust despite uncertainty in the $v = 0$ backward scattering region (see methods section below).

To examine these nonstatistical effects in more detail, we simulated the $^{18}O + {}^{32}O_2$ isotope exchange reaction using a QS model[18,19] and the QCT method[24] on the ab initio PES of Babikov et al.[13] Both methods were used to predict $P(\theta)$s and product rovibrational populations at $E_{coll} = 7.3$ kcal/mol; $P(E_t)$s were derived from these rovibrational populations using a Gaussian convolution method[25] to account for the width of the experimental E_{coll} distribution. The QS- and QCT-predicted $P(\theta)$s and $P(E_t)$s (Figure 2) were then used to simulate the laboratory-frame TOF data (Figures 3 and 4, respectively).

The QS model captures the major features of the experimental $P(E_t)$s, which peak near E_{coll}, as demonstrated by the QS calculation of the correct times for the TOF peaks (Figure 3) and the similarities between the QS-calculated and empirically derived $P(E_t)$s (Figure 2). However, the QS calculations underpredict the TOF data at long times (>175 μs) and therefore underestimate the production of highly rovibrationally excited $^{34}O_2$, which may indicate that $^{34}O_2$ exhibits a nonstatistical internal energy distribution. Furthermore, since the QS model assumes long-lived O_3*, the $P(\theta)$s are necessarily forward/backward symmetric, and thus the QS model cannot reproduce the nonstatistical forward scattering bias.

Like the QS model, the QCT calculations reproduce the peaks near E_{coll} in the TOF spectra (Figure 4) and yield similarly shaped $P(E_t)$s (Figure 2C−E). Since the QCT method results in more $^{34}O_2$ in the $v = 1$ state than the QS model (12.5% vs 8.3%, respectively), it better predicts the nonstatistical rovibrational distribution, specifically, more scattering at TOFs > 175 μs. However, the QCT method still underpredicts the slow side of the $v = 0$ TOF peak, indicating that it still underestimates highly rotationally excited $^{34}O_2$. Importantly, the QCT calculations predict a strong forward scattering bias for $v = 0$ and $v = 1$, a consequence of ~75% of the calculated reactive trajectories going through short-lived (<1 ps), nonstatistical complexes in which intramolecular vibrational redistribution is not complete. However, the QCT-predicted forward bias is larger than those in the empirical $P(\theta)$s (Figure 2A,B), as is also evident in comparison with the TOF data in Figure 4 where the QCT simulation overpredicts the $v = 0$ forward scattering (i.e., at 10°−20°) and underpredicts sideways scattering (i.e., at 35°−60°). Thus, although the QCT model correctly predicts the occurrence of nonstatistical effects, the nonstatistical forward bias is overestimated while the nonstatistical character of the rovibrational distribution is underestimated. The origins of the QCT-experiment discrepancies are not yet clear. The treatment of ZPE may contribute to the disagreement, but we note that the angular distributions are forward-biased with or without the ZPE-violating trajectories. This point will be discussed further in a future publication. Other potential factors include inaccuracy of the PES and electronic non-adiabatic effects.

Comparison of our experimental and theoretical results also yields important new insights into the $O_3(X^1A')$ PES. Although the $^{34}O_2$ product is rovibrationally hotter than the QS prediction, it has relatively little rovibrational energy compared to products

(24) Raff, L. M.; Thompson, D. L. The classical trajectory approach to reactive scattering. In *Theory of Chemical Reaction Dynamics*; Baer, M., Ed.; CRC Press: Boca Raton, FL, 1985; Vol. 3, p 2.
(25) Balucani, N.; Casavecchia, P.; Banares, L.; Aoiz, F. J.; Gonzalez-Lezana, T.; Honvault, P.; Launay, J. M. *J. Phys. Chem. A* **2006**, *110*, 817−829.

of other triatomic reactions with deep wells, such as $O(^1D) + H_2$, $S(^1D) + H_2$, and $N(^2D) + H_2$,[25,26] which all yield more internally excited products. This unique rovibrational distribution of O_2 is likely due to the structure of the PES[13] in the transition state region of the exit channel which is characterized by a submerged "reef" structure that becomes a dominant centrifugal barrier at large J and/or diatomic rotational quantum number j.[27] This results in a very narrow transition state that attenuates the reaction probability for highly rotationally excited products. In contrast, the aforementioned insertion reactions all feature rather broad transition states for complex dissociation. Although both the QS and QCT calculations for $O + O_2$ result in rovibrational energy distributions that peak at low energies and qualitatively match the experimental $P(E_t)$s, both sets of calculations also underestimate rovibrational energy compared to experiment. To improve agreement with experiment, a better characterization of the O_3 PES, including electronic nonadiabatic interactions, and a full quantum treatment of the dynamics are needed.

Finally, we note that, although the isotope exchange reaction takes place on the same potential energy surface as the ozone formation reaction, the exchange reaction may be dominated by dynamics that are not easily accessed in the formation reaction. For example, the isotope exchange reaction can proceed through short-lived O_3* complexes while the ozone formation reaction proceeds primarily through longer-lived O_3* complexes that survive long enough to be collisionally stabilized to O_3. Indeed, this expectation is consistent with our QCT calculations which show that at our experimental collision energy of 7.3 kcal/mol the majority of reactive trajectories for isotope exchange are impulsive and do not visit the depths of the ozone potential well. Since laboratory studies have shown that the unusual KIEs in ozone formation tend to decrease as the pressure of the third body increases,[28−30] which in turn suggests that long-lived O_3* complexes likely contribute more to the formation isotope effects than do short-lived O_3* complexes, this distinction between the dynamics of the isotope exchange reaction versus those for the formation reaction is likely important when considering the origin of the formation KIEs. Nevertheless, our results here for the $O + O_2$ isotope exchange reaction provide new benchmarks for future dynamics and PES computational studies needed to gain further insight into the origin of unusual KIEs for ozone formation.

Conclusions

In summary, we combined reactive scattering experiments and theoretical calculations for the $^{18}O + {}^{32}O_2$ isotope exchange reaction to investigate directly the existence and nature of any nonstatistical effects in O_3* formation and decomposition and to probe the O_3 PES. Our results demonstrate that this reaction involves a robust nonstatistical bias toward forward scattering at a collision energy of 7.3 kcal/mol, which cannot be reproduced in the QS model at all and which is predicted but overestimated by the QCT calculations. Further evidence for nonstatistical behavior is exhibited in a product rovibrational distribution that is hotter than the QS prediction. On the other hand, the reaction yielded products with minimal rovibrational excitation compared to other triatomic complex-forming reactions, which we conclude is likely due to the nature of the PES near the transition state. Both the QS and QCT theories overestimate this tendency toward rovibrationally cold products, demonstrating that improvements in electronic structural and dynamical treatments of this important system are required. Our scattering data should guide such improvements, while our observation of nonstatistical effects in the $O + O_2$ isotope exchange reaction provides the first direct experimental evidence that O_3* dynamics are not purely statistical. Thus, these results should ultimately facilitate a deeper understanding of the unusual, dynamically driven isotope effects in ozone formation and, more generally, the nature and consequences of nonstatistical energy flow in chemical reactions.

Experimental and Theoretical Methods

Experimental Details. The ^{18}O atomic beam (50% $O(^3P)$, 50% $O(^1D)$) had an average velocity of 2170 ± 4 m/s, a speed ratio of 28, and an angular divergence of ±4.5° fwhm and was produced by 157.6 nm photolysis of a skimmed molecular beam of $^{36}O_2$ (<0.1% ^{16}O) from a pulsed valve (50 psig backing pressure) oriented almost perpendicular to the reaction plane to minimize background from the trace $^{34}O_2$ impurity in the molecular beam. A spherical−cylindrical MgF_2 lens focused the 50−60 mJ output of a F_2 excimer laser (Lambda Physik, LPX 210i, 50 Hz) to a spot size of 3 mm × 4 mm to photolyze the $^{36}O_2$. The $^{32}O_2$ molecular beam had an average velocity of 783 ± 5 m/s, a speed ratio of 18, and an angular divergence of ±1.7° and was produced by a pulsed valve (50 psig backing pressure) and skimmed. Both beams passed through apertures in a He-cryocooled copper cold plate (∼20 K) that reduced background from ambient O_2 in the chamber. After the beams were crossed, the products were ionized by electron impact and $^{34}O_2$ was selected by a quadrupole mass filter and directed to a Daly detector coupled to a multichannel scaler, which recorded time-of-flight (TOF) with 1 μs resolution. The detector was rotated in the plane of the reaction to record TOF spectra at eight laboratory angles between 10° and 60° (with the ^{18}O beam defined as 0°), selected to best cover the center-of-mass angular distribution of the products but limited to ≤60° due to the large background from $^{34}O_2$ (at 0.4% natural abundance in the $^{32}O_2$ beam) at 90°.

The raw TOF spectra were corrected for the background $^{34}O_2$ that undergoes inelastic scattering with the O atomic beam by measuring the large $^{32}O_2$ inelastic scattering signal at each angle, scaling to the natural abundance of $^{34}O_2$, and then subtracting this scaled background from the raw $^{34}O_2$ TOF spectra; the correction ranged from 6% of the $v = 0$ signal height at 10° to 48% at 60°. The data were also rebinned to 3 μs to improve the signal-to-noise ratio.

Theoretical Methods. The QS model is based on a statistical treatment of reactive scattering assuming a long lifetime of the reaction intermediate. In particular, the state-to-state reaction probability is given as: $P_{f\leftarrow i} = p_i^{(c)}p_f^{(c)}/\Sigma_l p_l^{(c)}$, where $p_{i,f}^{(c)}$ are respectively the quantum capture probabilities for the reactant (i) and product (f) channels, and the sum runs through all open channels.[31] The differential cross sections were obtained using a random phase approximation, which necessitates a forward−backward symmetry in the angular distribution. The quantum treatment of the capture processes allows an accurate description of quantum effects such as tunneling and zero-point energies. By design, however, the QS model is incapable of describing short time events but serves as a useful limiting case for long-lived complex-forming reactions.

(26) Casavecchia P. *Rep. Prog. Phys.* **2000**, *63*, 355−414.
(27) Grebenshchikov, S.Y.; Schinke R.; Fleurat-Lessard P.; Joyeux M. *J. Chem. Phys.* **2003**, *119*, 6512−6523.
(28) Morton, J.; Barnes, J.; Schueler, B.; Mauersberger, K. *J. Geophys. Res.* **1990**, *95*, 901−907.
(29) Thiemens, M. H.; Jackson, T. *Geophys. Res. Lett.* **1990**, *17*, 717−719.
(30) Guenther, J.; Erbacher, B.; Krankowsky, D.; Mauersberger, K. *Chem. Phys. Lett.* **1999**, 306, 209−213.
(31) Rackham, E. J.; Gonzalez-Lezana, T. D.; Manolopoulos, E. *J. Chem. Phys.* **2003**, *119*, 12895−12907.

The QCT calculations were based on the Newtonian mechanics with quantized initial conditions and carried out using a custom-designed version of the VENUS code.[32] While the QCT approach accounts for the full dynamics, its treatment of the zero-point energy and other quantum features such as resonances is often unsatisfactory.

Possible Interference from $O(^1D) + O_2$. Both theory and our experimental results rule out significant contributions to the observed signal from $O(^1D) + O_2$ isotope exchange due to the presence of $O(^1D)$ in the ^{18}O atomic beam. First, the quenching reactions $O(^1D) + O_2(X^3\Sigma_g^-) \rightarrow O(^3P) + O_2(X^3\Sigma_g^-)$, $(a^1\Delta_g)$, or $(b^1\Sigma_g^+)$ are exothermic by 46, 23, or 8 kcal/mol for the respective product O_2 electronic states and would therefore produce O_2 products much more energetic than observed. Furthermore, the relevant potential energy surfaces are all repulsive and cross either at energies above the collision energy or at long $O-O_2$ distances (>1.8 Å),[33] prohibiting isotope exchange. A second possible reaction, $^{18}O(^1D) + {}^{32}O_2 \rightarrow {}^{16}O(^1D) + {}^{34}O_2$, is also believed to be unimportant since $O(^1D) + O_2$ correlates with a repulsive electronically excited state of ozone[34] and therefore is not likely to undergo isotope exchange. Furthermore, experiments with a pure $^{18}O(^3P)$ beam from the photolysis of ^{18}O labeled SO_2 (but with poor speed resolution) produced more isotope exchange signal than the 50:50 beam of $O(^3P)$ and $O(^1D)$, allowing us to conclude that 100 ± 15% of the observed $^{34}O_2$ signal is from $O(^3P) + O_2$.

Uncertainty in Experimental Angular Distribution. The backward scattering region for the $v = 0$ channel is not well sampled by the experiment since good sampling of the $v = 0$ backward peak would require detection at laboratory angles that are too close to the $^{32}O_2$ beam and are therefore dominated by the natural abundance $^{34}O_2$. To verify that the TOF data require a forward bias, a second empirical fit was performed in which the $v = 0$ channel was constrained to be forward/backward symmetric, which resulted in an increased signal in the slower of the two TOF peaks at 60°. To compensate, the new fit required that the $v = 1$ channel have no backward peak. Thus, despite large uncertainties in the shape of the $P(\theta)$s in the backward scattering region, the data do in fact require a bias toward forward scattering in one or both channels and therefore do demonstrate nonstatistical character.

Acknowledgment. We gratefully acknowledge support to UC Berkeley from the U.S. National Science Foundation (ATM-0096504; Graduate Fellowships for A.V. and K.M.), the David and Lucile Packard Foundation, the Camille Dreyfus Teacher-Scholar Award, and the Berkeley Atmospheric Sciences Center (Fellowship for A.V.); to The Institute of Atomic and Molecular Sciences from Academia Sinica; to the University of New Mexico from the U.S. Department of Energy (DE-FG02-05ER15694); and to the Hungarian Academy of Sciences from the Hungarian National Scientific Research Fund (T 049257) and acknowledge experimental assistance from Chi-Wei Liang.

JA0668163

(32) Hase, W. L.; Duchovic, R. J.; Lu, D.-H.; Swamy, K. N.; Vande Linde, S. R.; Wolf, R. J. VENUS: A General Chemical Dynamics Computer Program, Quantum Chemistry Program Exchange Bulletin **1996**, *16*, 671.
(33) Miura, N.; Hashimoto, K.; Takahashi, K.; Taniguchi, N.; Matsumi, Y. *J. Chem. Phys.* **2002**, *116*, 5551−5556.
(34) Zhu, H.; Qu, Z-W.; Tashiro, M.; Schinke, R. *Chem. Phys. Lett.* **2004**, *384*, 45−51.
(35) Luther, K.; Lum, K.; Troe J. *Phys. Chem. Chem. Phys.* **2005**, *7*, 2764−2770.
(36) Ivanov, M. V.; Schinke, R. *J. Chem. Phys.* **2006**, *124*, 104303.